Astron. Astrophys. 356, 888–894 (2000)

ASTRONOMY
AND
ASTROPHYSICS

A chromospheric model for FU Ori

G. D'Angelo[1], **L. Errico**[1], **M.T. Gomez**[1], **L.A. Smaldone**[2], **M. Teodorani**[1], **and A.A. Vittone**[1]

[1] Osservatorio Astronomico di Capodimonte, Via Moiariello 16, 80131 Napoli, Italy
[2] Dipartimento di Scienze Fisiche, Mostra d'Oltremare Pad. 19, 80125 Napoli, Italy

Received 31 March 1999 / Accepted 1 March 2000

Abstract. We present medium and high-dispersion optical spectra of the FUOr variable FU Ori, demonstrating that some lines are subject to variability both on a yearly and on a daily time scale. Some raw models of accretion disk atmospheres are presented in order to explain both qualitatively and quantitatively the dynamics of the observed line variability. Computing synthetic profiles for the Hα line by using the non-LTE MULTI code, we find that the emission component of this feature is very sensitive to the temperature gradient and the maximum temperature reached in a chromospheric-like layer. Further, the blue absorption component of the Hα depends only on the velocity field of the wind and the transition between the absorption and emission components is produced where the chromosphere ends and the wind begins. Similar chromospheric analysis is applied to the profile of the Na I D lines in pure absorption.

Key words: stars: individual: FU Ori – stars: pre-main sequence – stars: chromospheres – stars: variables: general – line: profiles

1. Introduction

FU Ori is the prototype of a peculiar class of objects, named FUOrs, which represent the young and active phase of pre-main sequence stars and are characterized by an evolutionary age of 1–3$\times 10^5$ yrs, which is 50 times less than the age of classical T Tauri stars. A good general description of FUOrs properties has been presented by Herbig (1989), Reipurth (1990), Hartmann et al. (1993), Hartmann & Kenyon (1996) and Teodorani et al. (1998). Structural and dynamical configurations of FUOrs are defined by the presence of two basic features which are well known from spectroscopic observations: an accretion disk embedded in a protostellar IR-emitting dust cloud (Smith et al. 1982) and a bipolar outflow which departs perpendicularly to the disk. According to previous observations, supported by recent models, the accretion disk can be subject to strong perturbations which give rise typically to an eruptive increase of mass accretion from $\dot{M} = 10^{-8}$ M$_\odot$ to $\dot{M} = 10^{-5}$ M$_\odot$.

The eruptive behaviour of FU Ori was discovered by gathering together photometric data taken during over the past 50 years. The B light curve shows the evidence of a very fast nova-like increase of up to 6 magnitudes on a time-scale of about one year and a very long and smooth decay at high levels of brightness on a time scale of the order of decades (Herbig 1977; Kolotilov & Petrov 1985; Hartmann et al. 1993; Ibragimov 1993; Hartmann & Kenyon 1996).

Spectroscopic observations of FU Ori furnished an essential piece of evidence for the existence of an accretion disk surrounding the central star: the presence of low-excitation absorption lines characterized by a double-peaked profile whose separation increases when the wavelength decreases and which, according to models, resembles an optically thick disk pseudo-atmosphere (Hartmann & Kenyon 1985, 1987, 1996; Kenyon et al. 1988; Kenyon & Hartmann 1989; Welty et al. 1992 and Hartmann et al. 1993).

The alleged proof of the existence of an accretion disk in the object FU Ori, together with the observed eruptive characteristics, has led to the theoretical calculation that the observed fast-rise and long-decay light curve may be due to thermal instabilities (Bell et al. 1995) caused by a possible external gravitational perturbation which is able to trigger an initial inward directed ionization front (fast rise) followed then by an outward directed ionization front (long decay).

The P Cygni optical and UV line profiles, the strong blue-shifts recorded in some photospheric absorption lines present in the spectra of FU Ori and the differential shift behaviour of such profiles, suggest that this object has powerful, rapidly expanding and rotating, winds arising from the surface of the luminous accretion disk (Bastian & Mundt 1985; Ewald et al. 1986; Croswell et al. 1987; Kenyon & Hartmann 1989; Welty et al. 1992; Calvet et al. 1993; Hartmann & Calvet 1995; and Reipurth et al. 1996). Asymmetries detected in the optical and IR (CO features) absorption lines imply mass loss rates of $\dot{M} = 10^{-5}$ M$_\odot$ and $\dot{M} = 10^{-7}$ M$_\odot$ respectively, indicating that the inner disk regions, in this object, are more effective in ejecting material. Some P Cygni lines such as Na I D, Hα and CO IR absorptions are subject to a significant variation of both the width and the blue-shift of the absorption component on an apparent time scale of some years (Kenyon & Hartmann 1989). The absence of a detectable optical bipolar outflow and Herbig-Haro objects is probably due to the low amount of circumstellar

Send offprint requests to: Maria Teresa Gomez
Correspondence to: gomez@na.astro.it

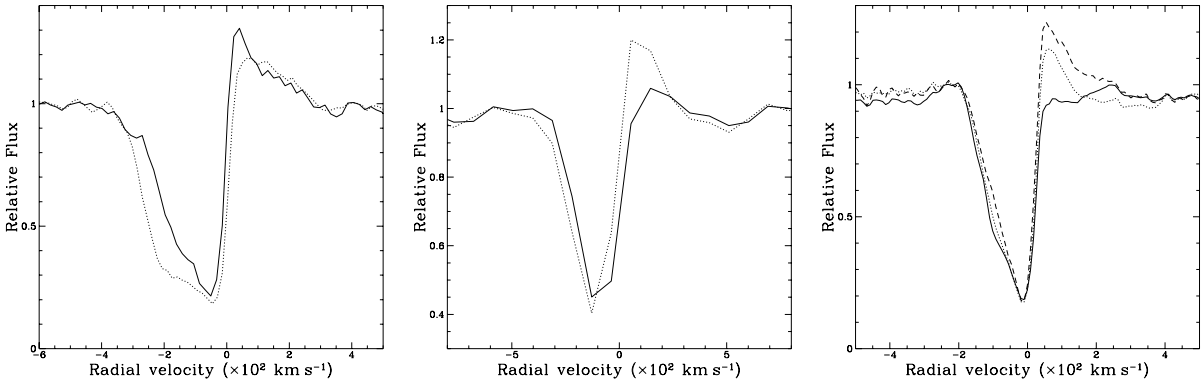

Fig. 1. Observed variations of the Hα profile of FU Ori. Left: year-to-year variations from medium-high dispersion spectra (Dec 7, 1990: full line; Jan 7, 1992: dotted line). Center: day-to-day variations from medium-dispersion spectra (Jan 14, 1997: full line; Jan 15, 1997: dotted line). Right: day-to-day variations from high-dispersion spectra (Jan 7, 1998: dashed line; Jan 8, 1998: dotted line; Jan 9, 1998: full line).

matter and the time history of the ejection (Hartmann & Kenyon 1996).

Aside from the reported long time scale eruptive behaviour, FU Ori is variable also on daily time scales both photometrically and spectroscopically. A cyclic component in the light curve with variations of the order of 0.1 mag on a time scale of about 10 days has been found by Kolotilov & Petrov (1985) and by Ibragimov (1993). Some evidence of daily variability is weakly present in the line profiles obtained by Croswell et al. (1987), even if no systematic day-to-day monitoring was done.

In this paper we shall devote our attention to three aspects of the FU Ori spectroscopic behaviour. First, we shall show the observational evidence of the year-to-year and day-to-day variability recorded in our medium and high-dispersion spectra, and speculate on possible causes. Secondly, we shall present our computation of synthetic profiles for Hα and the Na I D lines by using the non-LTE MULTI code (Carlsson 1986), given the assumptions that the optical spectral features are produced by an accretion disk atmosphere driven wind. Finally, we shall discuss how our chromospheric model is able to explain the observed line variability.

2. Observations

Our FU Ori spectra were obtained with three different types of telescopes and detectors. The journal of observations is given in Table 1. Spectra were obtained using the following instruments:

1. The 1.6 m Perkin-Elmer telescope of Pico dos Dias Observatory (Laboratorio Nacional de Astrofisica - Minas Gerais - Brazil) with the Coudé spectrograph (PDDCS) equipped with a CCD detector which allows the spectra to be recorded both on a 578-pixel (Dec 7, 1990) and on a 1152-pixel frame (Jan 7, 1992).
2. The 1.52 m Loiano telescope of Bologna Astronomical Observatory with the Bologna Faint Object Camera & Spectrograph (BFOSC) equipped with a CCD detector which recorded the spectra on a 1100-pixel frame.
3. The REOSC Echelle Spectrograph (RES) attached to the 1.82 m telescope located on Mt. Ekar in Asiago and operated by the Astronomical Observatory of Padova. In 1998 the RES spectrograph was equipped with a Thompson THX31156 UV-coated CCD detector, 1024×1024 pixels of 19 μm on a side.

Table 1. Journal of spectroscopic observations.

#	Date	Exp. (sec)	Wavelength (Å)	Dispersion (Å mm^{-1})	Instrument
1	1990 Dec 7	600	6510–6730	18.2	PDDCS
2	1992 Jan 7	600	6380–6800	18.2	PDDCS
3	1997 Jan 14	2400	6300–7100	26.0	BFOSC
4	1997 Jan 15	2400	6300–7100	26.0	BFOSC
5	1998 Jan 7	3600	6480–6670	4.5	RES
6	1998 Jan 8	3600	6480–6670	4.5	RES
7	1998 Jan 9	3600	4330–6670	3.1-4.5	RES

3. Spectroscopic variability

Our spectral analysis has been mostly concentrated on the study of the Hα line profile. Almost all Hα spectra acquired by previous authors show that this line is characterized by a P Cyg profile in which the ratio of the emission to the absorption component is largely less than 1. As an exception, the opposite behaviour (ratio of the order of 2.8) has been measured by Dibaj & Esipov (1968).

The FU Ori spectra we acquired confirm the generally observed situation: the Hα line is characterized by a P Cyg profile with a weak emission component and a very strong absorption component; such line profile is subject to drastic variations on both long and short time-scales.

3.1. Yearly time-scale

Medium-high dispersion spectra taken in 1990 and 1992 (see Fig. 1) show that the Hα line profile underwent the following changes:

1. The blue-shifted absorption component is characterized by a multiple structure. Its full width at half maximum (FWHM) was subject to a 50 km s^{-1} increase as a result of the increase of the depth of the bluest absorption peak.
2. The intensity of the emission component was subject to a 40% variation.

Moreover, by comparing the 1990–1992 spectra with the 1997 and 1998 data (see Fig. 1, Table 2), it is possible to observe that a further variation of the secular type is present in the absorption component of Hα, which appears to have been subject to a 50 km s^{-1} FWHM decrease from 1992 to 1998.

A similar variability of the P Cyg Hα absorption component can be seen by comparing previous spectra presented by Bastian & Mundt (1985), Croswell et al. (1987), Kenyon & Hartmann (1989), Welty et al. (1992), Hartmann & Calvet (1995) and Reipurth et al. (1996). Moreover, Kenyon & Hartmann (1989) first showed that the Na I D absorption is also subject to a strong width variation on a yearly time-scale. A compilation of measured FWHM values for the Hα absorption component and the Na I 5890 Å is presented in Table 2.

Strong analogous FWHM variations of both Hα and Na I D absorptions in the FUOr object Z CMa (Hartmann et al. 1989) have been recently discovered by Chochol et al. (1999).

3.2. Daily time-scale

Medium-dispersion spectra acquired in January 1997 and high-dispersion spectra acquired in January 1998 (see Fig. 1) show the following day-to-day profile changes:

1. The emission component was subject to a drastic amplitude variation. A gradual decrease followed by total disappearance was observed (see Fig. 1, central and right panel).
2. The FWHM of the absorption component was subject to only a slight change. This variation was not due to the variability of the emission component, but was mainly caused by a small but not negligible increase of the blue wing of the absorption component.
3. The central wavelength of the main absorption was not subject to any variation. In these spectra the filling-in effect due to the appearance of the emission component appeared to be totally ineffective in blue-shifting the main peak of the absorption component.

It is worth noticing that high-dispersion spectra obtained in 1998 (see Fig. 1, Table 2) show that the amplitude variation of the Hα emission component appears to be anti-correlated with the FWHM variation of the absorption component. The FWHM variations are well above 2 km s^{-1}, which is the r.m.s. error of the RES spectrograph at Hα with a good S/N ratio.

The evidence of short-term variability in FUORs is supported also by the recent study of a similar object, Z CMa, which demonstrated definitely that FUOrs can be subject to intermittent line profile variability on both daily and hourly time scales (Chochol et al. 1998).

Table 2. FWHM of Hα and Na I 5 890 Å P Cyg absorptions. Error on FWHM is 5–10%.

Date	Hα (km s^{-1})	Na I 5890 Å (km s^{-1})	Reference
1972 Mar 14	240		1
1981 Nov 8	200	105	2
1982 Nov 30		125	3
1984 Oct 10	185		3
1984 Dec 5	175		3
1984 Dec 7	185		3
1985 Feb 7	245	145	4
1985 Mar 7	160		3
1986 Dec 15	250	180	5
1987 Dec 29	190		6
1988 Jan 6	90	90	5
1988 Nov 30	195	110	7
1990 Dec 7	200		9
1992 Jan 7	255		9
1992 Dec 6		110	8
1997 Jan 14	205		9
1997 Jan 15	210		9
1998 Jan 7	115		9
1998 Jan 8	130		9
1998 Jan 9	140	145	9

1 = Zaitseva & Kolotilov (1973).
2 = Bastian & Mundt (1985).
3 = Croswell et al. (1987).
4 = Reipurth (1990).
5 = Kenyon & Hartmann (1989).
6 = Reipurth et al. (1996).
7 = Welty et al. (1992).
8 = Hartmann & Calvet (1995).
9 = The present paper.

4. Atmospheric modelling procedures

The presence of powerful accretion disks in FU Ori objects has been ascertained because many properties can be explained by the predicted emission of geometrically thin and optically thick disks. Furthermore, such outbursting objects can be treated as steady disks because, during epochs considerably after outbursts, the changes of the mass accretion rates are slower and the disk itself can shine strongly in the optical and near-IR spectral regions, completely overwhelming the stellar photospheric light.

It may be difficult to believe that a disk spectrum can look so much like the spectrum of a normal star with strong absorption lines, but similarities arise because both stellar atmospheres and FUOr-type disk atmospheres (especially those parts very close to the central stellar object) have comparable effective temperatures (Lynden-Bell & Pringle 1974) and surface gravities; furthermore, both systems passively transmit energy generated in a deep interior producing the outwardly decreasing temperature distribution necessary to have an absorption line spectrum.

In order to construct synthetic line profiles, we have modelled the accretion disk atmosphere of FU Ori ignoring the central star, whose photometric and spectroscopic effects on the

emerging spectrum are negligible (Hartmann & Kenyon 1985; Kenyon et al. 1988).

As in Calvet et al. (1991), we have characterized the FU Ori disk using the following parameters: $M_* = 0.49$ M$_\odot$, $R_* = 4.42$ R$_\odot$ and $\dot{M} = 1.59 \times 10^{-4}$ M$_\odot$yr^{-1}. According to these values, we have determined the effective temperature and surface gravity assuming a steady disk with hydrostatic equilibrium along the vertical direction (which is parallel to the rotational axis). We have then constructed a disk atmosphere, formed by a narrow photosphere and a wide expanding wind. While investigating the atmospheric properties able to roughly reproduce some of the observed spectral features and their variability, we have found it necessary to insert, between the photosphere and the wind, an intermediate layer with a temperature gradient inversion, similar to a stellar chromosphere. We have studied the effects of some free parameters of this thin layer on the emerging line profiles.

Since we were searching for some indications about the fundamental physical elements so that they could be used to build successively more detailed models, we have used the following simplifying approximations:

1. the accretion disk was considered as standing "pole-on" (i.e. the rotational axis points towards us);
2. we used a plane-parallel geometry, which represents the most simple approximation of the cylindrical geometry proposed by Calvet et al. (1993), to treat the whole atmosphere (photosphere, chromosphere and wind);
3. finally, we only took into account the effects of those parts of the disk responsible for the production of the spectroscopic features we were mostly interested in, namely Hα and Na I D, and which we present in this paper.

For the accretion disk photosphere, we built models having temperature and electronic density height distribution selected from Kurucz grids of stellar models (Kurucz 1993), with the appropriate $T_{\rm eff}$ and $\log g$ values. Atomic abundances were fixed as being equal to the solar case (Anders & Grevesse 1989) and microturbolence was defined to be equal to 2.0 km s^{-1}. Wind temperature distribution has been considered almost isothermal (Croswell et al. 1987) with values never higher than 5000 K, while a positive gradient was imposed to the velocity field. We allowed the velocity field to range from a zero value, corresponding to hydrostatic photospheric layers, to maximum values of 250–450 km s^{-1} (depending on the amount of blue-shift measured in the absorption component of Hα line). In the layers where the velocity field is different from zero, mass conservation was enforced by keeping constant the quantity ρv_z (where v_z is the velocity component along the z axis), as requested by the plane-parallel geometry.

For the line synthesis of Hα and Na I resonance lines we used version 2.2 of the MULTI code (Carlsson 1986), in order to solve the radiative transfer problem in non-local thermodynamic equilibrium and in a unidimensional expanding atmosphere. The adopted atomic models are formed by six bound levels plus a continuum in the case of hydrogen atom and eleven bound levels plus a continuum in the case of sodium atom. Every level is collisionally coupled to each other level. Radiative transitions from ground state to continuum as well as bound–bound transitions are treated in detail. The other transitions are treated with a radiation temperature. Kurucz models provide the starting distribution of temperature, electron density and velocity. The electron density is then iteratively updated, following the kinetic equilibrium of Hydrogen. The wind temperature and velocity are semiempirically modified in order to obtain the best agreement with the observed line profiles.

The accretion disk has been divided into rings of finite radial extent, however we noticed that Kurucz models with $T_{\rm eff}$ and $\log g$, differing by less than 1000 K and 0.5 respectively, do not produce sensitive differences on the line profiles because of our simplifying approximations. So we have chosen, as radial extent of each annulus, a quantity Δr such that a disk portion is covered where maximum variations of $\Delta T_{\rm eff} = 1000$ K and $\Delta \log g = 0.5$ exist. The central values are used as the ring effective temperature and surface gravity.

By considering only the spectral contribution of one annulus, having an atmosphere formed by a photosphere and a wind layer, we obtain good results in reproducing the blue shifted wing of Hα. We found that the absorption intensity and the width of line profile are sensitive to the photospheric effective temperature as well as to the value of temperature of the (isothermal) wind. The formation depth of the line corresponds roughly to the upper boundary of the photospheric layer, where this layer connects to the wind and where a smaller value of wind temperature produces a deeper core. The asymmetry in the blue portion of the profile is reproduced by adopting a positive velocity gradient in the wind so that the gas speed grows almost linearly with respect to the quantity $\left[\log \int_z^\infty \rho dz\right]$. The ring which best reproduces the observed spectra has a photospheric $T_{\rm eff} = 5\,000$ K and $\log g = 1.0$.

The red portion of the profile is not altered by the temperature and velocity field of the wind. In order to reproduce the emission component it is necessary, with this geometry, to insert a chromospheric layer at the junction between the photosphere and the wind in the atmospheric model. The chromospheric layer has been modelled as a layer in hydrostatic equilibrium.

We found that the emission component is very sensitive to the temperature gradient as well as to the maximum value of temperature reached in the chromospheric layer (Fig. 2, Panels A and B); in contrast the blue absorption component of the profile depends only on the velocity field of the wind (Fig. 2, Panel C). We also noticed that the transition between absorption and emission takes place where the chromosphere ends and the wind begins, that is where the gas starts to expand.

Nevertheless, a single annulus, even with such an atmospheric stratification, cannot reproduce exactly the blue and the red part of Hα profile, i.e. it is not possible to match, at the same time, the absorption and the emission peaks.

Better results can be achieved by using two rings for the disk: a hotter one with $T_{\rm eff} = 5\,000$ K ($\log g = 1.0$) and a cooler one with $T_{\rm eff} = 4\,000$ K ($\log g = 0.5$). The cooler ring represents the neighbouring external annulus. Each annulus has an atmosphere with the combined stratification photosphere,

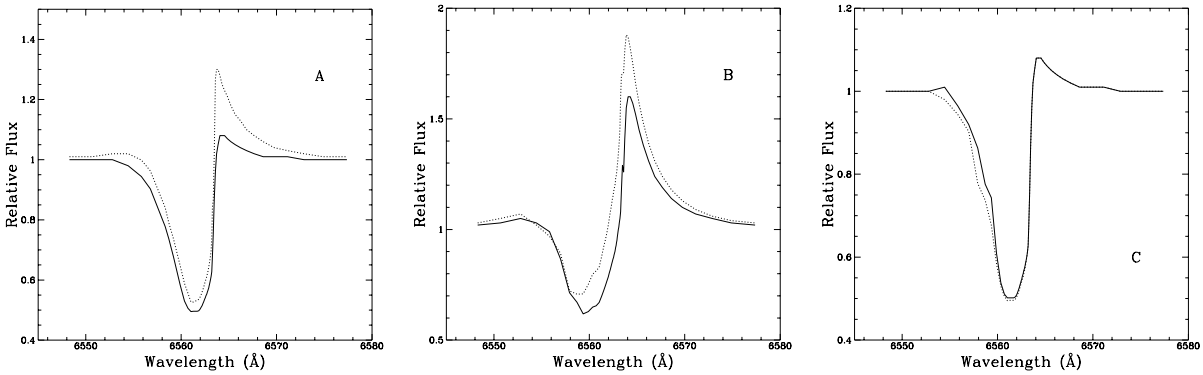

Fig. 2. Here there are three samples of Hα synthetic profiles. They show the line sensitivity to the chromospheric temperature distribution (Panel A and B) and to the wind velocity field (Panel C). Panel A contains two profiles generated by identical atmospheric models except for the maximum value of chromospheric temperature: 6 250 K (solid line) and 8 000 K (dash line). A similar situation is drawn in Panel B where the top values of 11 000 K (solid line) and 15 000 K (dash line) are attained in the chromospheric layer. Finally, Panel C displays the profiles produced by two models with asymptotic wind speeds of 370 km s^{-1} (solid line) and 390 km s^{-1} (dash line).

chromosphere and wind. Both rings have quite similar wind velocity fields. The wind temperature of the cooler component is set to 3 000 K while the chromospheric temperature is never higher than 7 000 K. The emerging line spectrum $F_R(\lambda)$ (flux relative to the continuum) results from the contribution of both rings, according to the following mean:

$$F_R(\lambda) = \frac{\sum_i (r_{i+1}^2 - r_i^2) f_i(\lambda) B(T_i)}{\sum_i (r_{i+1}^2 - r_i^2) B(T_i)}$$

where r_i is the inner annulus radius, $f_i(\lambda)$ is the normalized flux as computed by MULTI code and $B(T_i)$ represents the Planck function relative to the temperature T_i and the central wavelength of the spectral line. As regards the Hα line, in the framework of our simplifying approximations, using more than two annuli does not seem to improve the agreement of the synthetic profiles with the observed ones.

In this way we were able to produce a satisfactory fit for the P Cygni profiles of Hα (Fig. 3) and the complex blue shifted absorption of the Na I resonance lines (Fig. 4). Anyway, it must be pointed out that from the computational point of view, while modelling the Hα, we found it to be a difficult task to connect different atmospheric layers where the profile itself presents a sharp discontinuity. In fact the resultant steep gradient of temperature added to the non-hydrostatic equilibrium can produce numerical troubles in the computing code.

5. Discussion

Among our data we note a large variability of the Hα profile, not only in the blue absorption component but also in the red emission component as well. We are able to reproduce the former essentially by changing the maximum temperature value and the relative gradient of the chromospheric layer while the latter is reproduced by imposing a suitable velocity distribution in the wind.

Even during apparently quiescent states, the wind produced by this object is not constant. It seems to be characterized by "replenishment phases" alternating with "depletetion phases" on a time-scale on the order of one or more years. This can be noted in the large variation of the FWHM of the Hα absorption component (see Fig. 1, Table 2), which causes a subsequent variation of the equivalent width, occurring on a time interval of the order of some years.

When we deal with the daily observations, the wind does not seem to show any variation in velocity and temperature (see Fig. 3), in the case of January 1998 (high resolution) data. However in the case of January 1997 lower resolution observations, the asymptotic wind speed shows an increase of 60 km s^{-1} in one day.

In both cases there are strong variations of the emission component, which is clearly evident even in such a limited data set. The intensity variation of the emission peak, which is produced by a thin chromospheric layer in our model, can be explained mainly by its temperature variation. From the 14$^{\text{th}}$ through the 15$^{\text{th}}$ of January 1997 we detect, according to the models, a temperature increase of the order of 3 000 K, whereas in January 1998, we have observed a cooling phase, of the order of 10 500 K.

In this case we may argue that the different wind speed behaviour as well as a correlation, between the FWHM of the absorption component and the emission component intensity, are related to two different phases: a heating and a cooling one. We should emphasize that the observed anti-correlation between the FWHM and the emission component was possible due to the high spectral resolution.

Most of the variability of FU Orionis can be explained assuming the existence of a mechanism able to change the thermodynamic state of the chromosphere itself. It is not difficult to suppose, in the scenario of FU Orionis objects, the existence of thermal instabilities and to hypothesize an energy release that generates a time variable chromosphere. Furthermore in our model the chromosphere is a thin layer with a very low thermal capacity, so its variability is effective on the line profile in short time intervals. The response of the wind is strongly related to the rising and falling of the *perturbation* and to its physical nature. Nevertheless, a semiempirical model simply relies on some ba-

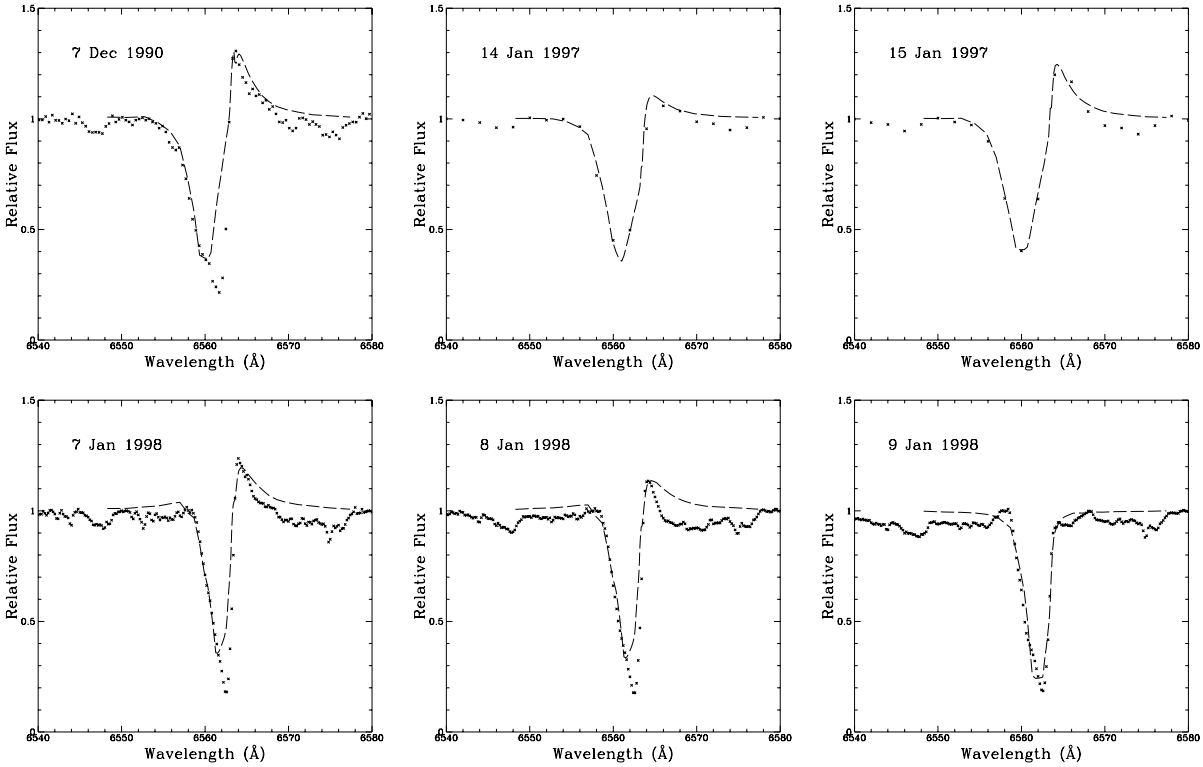

Fig. 3. Hα fitting (dash line) to different epoch observations (crosses). All the synthetic profiles come from a two-ring atmosphere with three layers each. The first (7 Dec 90) observation was reproduced imposing a chromospheric maximum temperature of $18\,000$ K and an asymptotic wind speed of 450 km s^{-1}. The second (14 Jan 97) observation was matched by using the corresponding values of $8\,000$ K and 390 km s^{-1}, while the third (15 Jan 97) required values of $11\,000$ K and 450 km s^{-1}. The last three observations (7, 8, 9 Jan 98) were reproduced adopting the same wind velocity field, with an asymptotic value of 250 km s^{-1}, and the following values for the top chromospheric temperature: $18\,000$ K, $15\,000$ K and $7\,500$ K.

sic observational features; so they depend *neither* on the kind of energy source which should be responsible for the change of plasma physical conditions in the disk *nor* on the theory which could explain the nature of this source.

6. Conclusions

The possible existence of a layer, with a temperature gradient inversion, in the atmosphere of FUOrs was first suggested, but not applied in their models, by Croswell et al. (1987) even though they did not treat these systems as accretion disks.

So far, many people have used a disk atmosphere to reproduce some spectral features of these objects (for example Calvet et al. 1991, 1993) but none has studied the optical lines we have tried to reproduce.

We propose, for the FU Ori disk atmosphere, a structure based on a narrow photosphere and a wide expanding wind separated by a thin intermediate layer with a temperature gradient inversion, much like a stellar chromosphere. The spectroscopic variability of FU Ori and, by extension, of FUOr objects can be explained in term of the variability in the wind and chromosphere.

The approximations used are quite coarse: only two contiguous rings of the accretion disk, a "pole-on" disk, plane-parallel geometry, photosphere and chromosphere in hydrostatic equilibrium. Nevertheless, this rough model is able to reproduce the most relevant aspects of Hα profile variability. It indicates the different behaviour of the wind during the chromospheric heating and cooling phase. It is unable, of course, to account for the observed anti-correlation between the Hα emission component and the FWHM of the absorption: this would imply a more sophisticated treatment of the region between the chromosphere and the wind, where the approximations used here are inadequate (mainly the hydrostatic equilibrium imposed on the chromosphere). This model can, however, be the starting point for a more realistic modelling.

From the observational point of view, a lot of work still should be done in terms of time coverage and temporal and spectral resolution. As shown, the modelling can take into account slight variations of the line profiles in order to provide large insights into the atmospheric structure. High resolution, both temporal and spectral, data can help to determine the "heating" mechanism (shock front?).

Is the long-term morphological variability in the blue-shifted absorption component of Hα real or is it due to the sparse observations? Is the observed short-term variability of a periodic nature?

The answers to these questions can be of fundamental value in understanding the physics of FUOr objects. The only way to

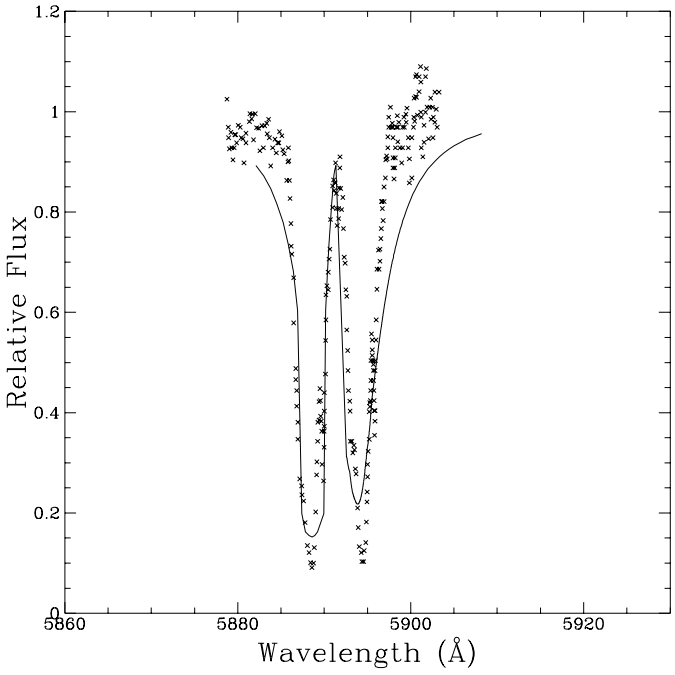

Fig. 4. The Na I resonance lines (crosses), as observed on September the 5-th 1981 (Bastian & Mundt 1985), and the fitting synthetic profile (solid line). In this case the maximum chromospheric temperature is equal to 6 000 K and the asymptotic wind velocity is 400 km s^{-1}. The match was carried out trying to reproduce the blend between the D_1 and D_2 lines.

answer these questions is to carry out very fequent, continuous observations with high spectral resolution.

Acknowledgements. The authors are indebted to Dr. C.A.O. Torres of Laboratório Nacional de Astrofísica/CNPq/MCT, Itajubá, Brazil, for furnishing spectra. Through the suggestions and the punctilious work of the anonymous referee, this paper earned clarity and deepness. We thank him for his contributions.

References

Anders E., Grevesse N., 1989, Geochimica et Cosmochimica Acta 53, 197
Bastian U., Mundt R., 1985, A&A 144, 57
Bell K.R., Lin D.N.C., Hartmann L., Kenyon S.J., 1995, ApJ 444, 376
Calvet N., Hartmann L., Kenyon S.J., 1991, ApJ 383, 752
Calvet N., Hartmann L., Kenyon S.J., 1993, ApJ 402, 623
Carlsson M., 1986, A computer program for solving MULTI-level non-LTE radiative transfer problems in moving or static atmospheres. Report No. 33, Uppsala Astronomical Observatory, Uppsala
Chochol D., Teodorani M., Strafella F., Errico L., Vittone A.A., 1998, MNRAS 293, L73
Chochol D., Teodorani M., Errico L., et al., 2000, MNRAS in press
Croswell K., Hartmann L., Avrett E.H., 1987, ApJ 312, 227
Dibaj E.A., Esipov V.F., 1968, In: Detre L. (ed.) Non-Periodic Phenomena in Variable Stars. Academic Press, Budapest, p. 107
Ewald R., Imhoff C.L., Giampapa M.S., 1986, In: New Insights in Astrophysics. UCL, London, ESA SP-263, p. 205
Hartmann L., Calvet N., 1995, AJ 109, 1846
Hartmann L., Kenyon S.J., 1985, ApJ 299, 462
Hartmann L., Kenyon S.J., 1987, ApJ 312, 243
Hartmann L., Kenyon S.J., 1996, ARA&A 34, 207
Hartmann L., Kenyon S.J., Hewett R., et al., 1989, ApJ 338, 1001
Hartmann L., Kenyon S., Hartigan P., 1993, In: Levy E.H., Lunine J.I. (eds.) Protostars and Planets III, University of Arizona Press, p. 497
Herbig G.H., 1977, ApJ 217, 693
Herbig G.H., 1989, In: Reipurth B. (ed.) ESO Workshop on Low Mass Star Formation and Pre-Main Sequence Objects. p. 233
Ibragimov M.A., 1993, Astron. Rep. 37, 176
Kenyon S.J., Hartmann L., 1989, ApJ 342, 1134
Kenyon S.J., Hartmann L., Hewett R., 1988, ApJ 325, 231
Kolotilov E.A., Petrov P.P., 1985, SvA Lett. 11, 358
Kurucz R.L., 1993, ATLAS9 Stellar Atmospheres Programs. CD-ROM No. 18
Lynden-Bell D., Pringle J.E., 1974, MNRAS 168, 603
Reipurth B., 1991, In: IAU Symposium 137, Flare Stars in Star Clusters, Associations, und Solar Vicinity eds. Mirzoyan L.V., Pettersen B.R., Tsvetkov M.K., Kluwer Dordrecht, p. 229
Reipurth B., Pedrosa A., Lago M.T.V.T., 1996, A&AS 120, 229
Smith H.A., Thronson H.A. Jr., Lada C.J., et al., 1982, ApJ 258, 170
Teodorani M., Errico L., Vittone A.A., 1999, Multifrequency Behaviour of FU Orionis Objects. Mem. Soc. Astron. Ital. 70, 959
Welty A.D., Strom S.E., Edwards S., Kenyon S.J., Hartmann L., 1992, ApJ 397, 260
Zaitseva G.V., Kolotilov A., 1973, Astrofizika Vol. 9, No. 2, 185